COMPARATIVE YIELDS OF ALKALI ELEMENTS AND THALLIUM FROM URANIUM IRRADIATED WITH HIGH-ENERGY PROTONS, ^{3}He and ^{12}C

H.-Å. Gustafsson, T. Bjørnstad*), B. Jonson, O.C. Jonsson, V. Lindfors**), S. Mattsson, A.M. Poskanzer†), H.L. Ravn and D. Schardt

The ISOLDE Collaboration, CERN, Geneva, Switzerland

Abstract

Mass-separated ion beams of the alkali elements Na, K, and Fr, and of the element Tl were produced by bombarding a uranium target with 600 MeV protons, 890 MeV $^3He^{2+}$, and 936 MeV $^{12}C^{4+}$. Isotopic production yields are reported. In the case of the ^{12}C beam these are thick target yields. Absolute cross-sections for the proton-beam data were deduced by normalizing the delay-time corrected yield curves to measured cross-sections. For products farthest away from stability the $^3He^{2+}$ beam generally gives the highest yields.

1. Introduction

The present work was initiated by the new possibilities of accelerating heavy ions at the CERN Synchro-cyclotron (SC). In addition to the 600 MeV proton and 910 MeV $^3He^{2+}$ beams, the SC is also able to accelerate $^{12}C^{4+}$ ions to an energy of 86A MeV. Since neutron emission usually is favoured relative to the emission of charged particles, the heavy-ion reactions may be suitable for the production of a variety of very neutron-deficient nuclides of Z higher than the target element. The purpose of the present experiment was, however, to investigate the production of nuclei lighter than the target and to see if the more complex projectiles have higher cross-sections so as to broaden significantly the isotopic-yield distributions.

A survey of comparative yield measurements for the elements Na, K, Tl, and Fr, produced by bombardment of 12 g U/cm^2 targets, was carried out at ISOLDE[1]). The ^{12}C ions are completely stopped in such thick targets, and therefore these measurements are thick target yields. Relative to protons and ^{3}He, the effective target thickness is thus reduced considerably. Here we shall discuss some aspects of the utilization of heavy ions for the production of rare nuclear species.

2. Experimental techniques

Data for the available projectiles at ISOLDE from the CERN 212 cm Synchro-cyclotron are summarized in Table 1. The beam intensities were measured by a secondary emission chamber which was calibrated against the reaction[2]) ^{27}Al(X,xnyp) ^{24}Na.

Table 1

Summary of beam data at the ISOLDE target

Projectile	Beam intensity (pμA) a)	Incident beam energy (MeV)	Energy loss in target (MeV)
p	3	600	30
$^3He^{2+}$	0.5	890	200
$^{12}C^{4+}$	0.1	936	936

a) 1 pμA = 1 particle microampère = 6.24 × 10^{12} particles/s.

The reaction products separated in the ISOLDE electromagnetic mass separator were brought through a beam-handling system onto a movable aluminized mylar tape[3]). The collected activity was transferred to a thick, 40 mm diameter, 4π plastic scintillator[4]), where the β-particles were counted. The detection efficiency of this detector was measured by means of standard β sources. The 4π plastic scintillator was also used for the Tl isotopes, which decay by isomeric transition or electron capture. In these cases, the absolute yields are estimated to be uncertain by a factor of 2 to 3 owing to the different efficiency of the β detector. The relative yields for the different projectiles are, however, not affected. For the detection of α-particles, silicon surface barrier detectors[5]) were used either placed in the beam behind a carbon collector foil or in combination with a tape-transport system[6]). The neutron-rich nuclides, which are characterized by the emission of β-delayed neutrons, were identified with a 4π neutron counter[7]) calibrated with a 48 g sample of uranium. For a few nuclides the gamma-rays were measured with a 17% Ge(Li) standard efficiency detector[7]). The observed counting rates were corrected for decay losses by using the formula presented in Bjørnstad et al.[8]) in order to obtain the saturation yields. To eliminate the effect of short-time variations in the bombarding beam intensity and the separator efficiency, most of the yields were obtained as ratios between two adjacent masses. The determined saturation yield ratios were then normalized to one absolute yield measurement for each element.

3. Results

The presented production yields from the proton and ^{3}He irradiations are normalized to a beam intensity of 1 pμA and a target thickness of 10 g U/cm^2, i.e. thin target yields. Since the ^{12}C beam is completely stopped in the target, its saturation yields are thick target yields normalized to 1 pμA. The proton-beam results are shown in Figs. 1-4. The isotopic distributions, shown in these figures, reveal within the experimental accuracy no structure due to odd-even effects. The Fr and Tl yields have their maxima at the neutron-deficient side of stability as expected for spallation products[9]). The yields for Na and K are peaked at the neutron-rich side, but closer to the stability line in accordance with the fragmentation model[9]). The yields from the ^{3}He and ^{12}C irradiations are presented in Figs. 5-12 as ratios to the proton-induced yields. The presented distributions will be further discussed in Section 4. The yields depend very strongly on the performance of the actual target-ion source system and, in order to keep the experimental conditions approximately the same, the presented data for p and ^{3}He were obtained by using the same target unit. The performances of various targets due to temperature differences mainly affect the short-lived nuclides because of their strong sensitivity to decay losses in the target. Occasionally 10-100 times higher yields have been observed for these nuclides. This means that precise cross-section measurements are difficult to

*) Present address: Department of Nuclear Chemistry, University of Oslo, Oslo, Norway.
**) Present address: Department of Physics, University of Helsinki, Helsinki, Finland.
†) Present address: Lawrence Berkeley Laboratory, Berkeley, Calif., USA.

perform at an on-line separator like ISOLDE but it is very suitable for relative yield measurements. It may still be interesting to estimate approximate cross-sections far away from stability, since it is very difficult to get this information from other techniques than on-line measurements. In order to obtain absolute formation cross-sections, the saturation yields have to be corrected for decay losses in the target. The parameter μ for the diffusion mechanism(s) in solids, described in Carraz et al.[10] was fitted to the experimentally measured diffusion curve for Na, thus giving a value of 0.26 s^{-1}. Earlier results from on-line measurements[10] show that the same μ value is roughly applicable also for K and Fr. The diffusion time for Tl was not measured for the actual target system, but earlier experiments have shown that it is much longer than for the alkalis and therefore the Tl yields were not corrected for delay in the target. The delay-corrected yields were then related to cross-sections measured by radiochemical methods[11-13]. The cross-sections given in Figs. 1, 2, and 4 are determined to a precision of a factor of 2 to 3, depending on the uncertainties in the delay-time corrections and the normalization cross-sections.

4. Discussion

For the fragmentation product Na, the yield ratios in Figs. 5-6 show that both ^{3}He and ^{12}C give a higher yield at the neutron-deficient as well as the neutron-rich side of the distributions. The higher yields are tentatively understood in terms of higher energy deposition in the target nucleus. For production purposes the ^{3}He beam will become even more attractive in the near future because a beam intensity of the same order as the proton beam is within reach at the SC. An unexpected high yield was observed for ^{21}Na with ^{12}C as projectile. To investigate if this could be attributed to the reaction ^{12}C on carbon in the target, a separate experiment with ^{12}C on a pure graphite target was performed. The result obtained was in agreement with integration of the 30 to 80 MeV ^{12}C on ^{12}C data[14,15] showing that the ^{21}Na is produced near the end of the range of the beam in the target. This experiment points to the possibility of performing such reactions in thick targets, which may be interesting in order to produce neutron-deficient nuclei in the region $Z < 20$ where suitable high-temperature targets for proton and ^{3}He bombardment are hard to find. In the ^{12}C on ^{12}C experiment a small contribution at masses $A > 24$ was also observed, originating from reactions with the Ta target container.

The ratios for the fragmentation product potassium, K, are shown in Figs. 7-8. The trend of higher yields from the ^{3}He and ^{12}C irradiations is not as pronounced as for Na, but still there is a gain in yield at both the neutron-deficient and neutron-rich sides of the distributions. The argument used above for the Na ratios is also applicable in this case to explain the higher yields produced in the ^{3}He and ^{12}C irradiations.

For the deep spallation product Tl, higher yields are expected when using ^{3}He or ^{12}C as projectiles instead of protons, because the higher total energy transferred to the system favours the evaporation of many particles. The effect is shown in Figs. 9-10. The experimental ratio illustrated in Fig. 9 shows that the yields for $A < 187$ are 10 to 100 times higher from ^{3}He than from protons. When using ^{12}C instead of protons as projectiles the effect is not that pronounced but still there is a gain in yield, as shown in Fig. 10. The measurements of the Tl isotopes were not extended to the neutron-rich side of stability because of contamination from the isobaric Fr isotopes.

In the case of the close spallation product Fr, Figs. 11-12, the higher bombarding energy of the ^{3}He and ^{12}C beams disfavours the yields. This is analogous to the case where the proton energy is increased from medium to high energy, where the cross-section decreases for close spallation products but increases for deep spallation and fragmentation products[9]. In the fission region the cross-section is rather unaffected by the higher bombarding energy in agreement with observations for Cs and Rb isotopes produced in 910 MeV ^{3}He irradiations[8]. For the most neutron-deficient nuclides, shown in fig. 11, there is a gain by using ^{3}He as projectiles, while nuclides closer to stability are disfavoured. This gives, because of contamination from neighbouring masses in the separator cleaner conditions when studying nuclear properties in the very-light Fr isotopes. The low ratio shown in Fig. 12 is not only a consequence of the reaction mechanism but also an effect of the small effective target thickness for ^{12}C, while the proton and ^{3}He yields are thin target yields.

During the ^{12}C experiment an attempt was made to produce elements heavier than the target. The effort was to produce Am isotopes by irradiating UC_2-graphite cloth by ^{12}C, which involves a transfer of three protons to the target nucleus. In this experiment a thermal ion source was used. The detection system was optimized to measure both alpha and fission-fragment energies. The most typical characteristic of the Am isotopes would be spontaneous fission, but no such events were observed. It is possible that relatively high-temperature stable Am compounds were formed, thus preventing the release of Am from the target. However, some weak alpha peaks were observed in the expected region of energy for Am. Assigning these alpha peaks to Am, an estimated upper limit of 30 μb for the production of ^{237}Am could be made, which roughly agrees with the data obtained by a low-energy ^{12}C beam[16].

The present work shows that the results obtained with the ^{3}He beam are very encouraging and higher production yields are established, especially for the deep spallation and fragmentation products. For production purposes the ^{3}He beam will become even more attractive with the planned higher beam intensity. The ^{12}C beam seems to offer no advantage for production of elements lighter than the target. The higher energy available does not compensate for its low intensity and shorter range as compared to ^{3}He and protons.

References

1) H.L. Ravn, L.C. Carraz, J. Denimal, E. Kugler, M. Skarestad, S. Sundell and L. Westgaard, Nucl. Instrum. Methods 139, 267 (1976).

2) J.W.N. Tuyn, R. Deltenre, C. Lamberet and G. Roubaud, CERN Internal Report HS-RP/TM/80-5.

3) A. Lindahl, O.B. Nielsen and I.L. Rasmussen, Proc. Int. Conf. on the Properties of Nuclei far removed from the Region of Beta Stability, Leysin, Switzerland, 1970, CERN 70-30 (1970), Vol. 1, p. 331.

4) H.L. Ravn, S. Sundell, L. Westgaard and E. Roeckl, J. Inorg. Nucl. Chem. 37, 383 (1975).

5) E. Hagberg, P.G. Hansen, J.C. Hardy, B. Jonson, S. Mattsson and P. Tidemand-Petersson, Nucl. Phys. A293, 1 (1977).

6) Ph. Dam, E. Hagberg and B. Jonson, Nucl. Instrum. Methods 161, 427 (1979).

7) T. Bjørnstad, H.-Å. Gustafsson, P.G. Hansen, B. Jonson, V. Lindfors, S. Mattsson, A.M. Poskanzer and H.L. Ravn, Nucl. Phys. A359, 1 (1981).

8) T. Bjørnstad, L.C. Carraz, H.-Å. Gustafsson, E. Hagberg, J. Heinemeier, B. Jonson, O.C. Jonsson, V. Lindfors, S. Mattsson and H.L. Ravn, New targets for on-line mass separation of nuclei formed in 600 MeV photon and 910 MeV ^{3}He reactions, to be published in 10th Int. Conf. on Electromagnetic Isotope Separators and Techniques related to their Applications, Zinal, Switzerland, 1980, in press.

9) R. Wolfgang, E.W. Baker, A.A. Caretto, J.B. Cumming, G. Friedlander and J. Hudis, Phys. Rev. 103, 394 (1956).

10) L.C. Carraz, S. Sundell, H.L. Ravn, M. Skarestad and L. Westgaard, Nucl. Instrum. Methods 158, 69 (1979).

11) I. Haldorsen, S. Engelsen, D. Eriksen, E. Hagebø, T. Johansen and A.C. Pappas, Production of ^{24}Na and ^{28}Mg by interaction of U with 15 to 600 MeV protons, J. Inorg. Nucl. Chem., in press.

12) H.L. Ravn, J. Inorg. Nucl. Chem. 31, 1883 (1969).

13) A.L. Lavrukhina and S. Rodin, Radiokhimiya 2, 83 (1960).

14) M. Conjeaud, S. Gary, S. Harar and J.P. Wieleczko, Nucl. Phys. A309, 515 (1978).

15) M.N. Nambrodiri, E.T. Chulik and J.B. Natowitz, Nucl. Phys. A263, 491 (1976).

16) E.L. Hyde, I. Perlman and G.T. Seaborg, The nuclear properties of the heavy elements (Prentice Hall, Englewood Cliffs, New Jersey, 1964), vol. 1, p. 350.

17) The ISOLDE Collaboration, The ^{49}K beta-strength function, to be published in Phys. Lett. B.

* * *

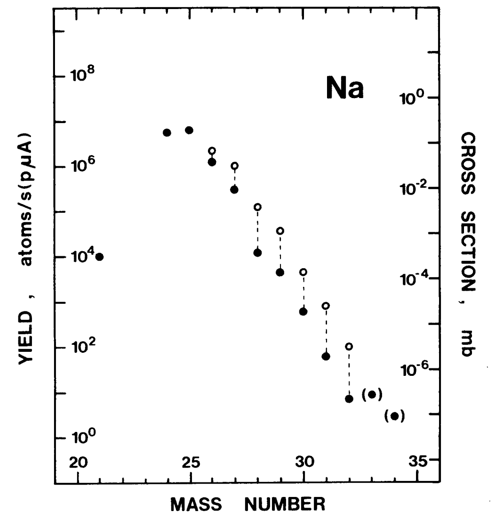

Fig. 1 Production yields of Na isotopes. Filled circles are normalized saturation yields (see text). The P_n values used are normalized to the new P_n value for ^{9}Li of (50 ± 4)% [7]. The cross-section scale on the right-hand axis is normalized to 0.19 mb measured[11] for ^{24}Na. This scale applies to the decay-corrected yields (open circles) according to the text. The points at masses 33 and 34 are within parentheses because the correction for the daughter activities is not taken into account.

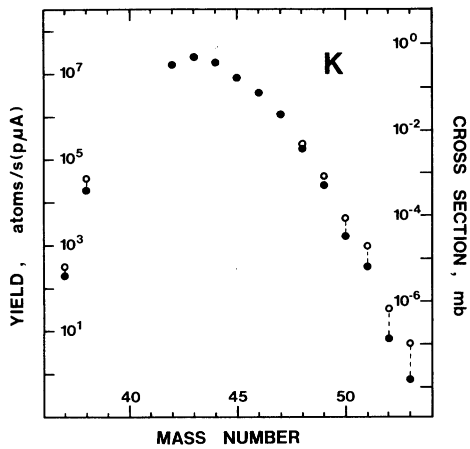

Fig. 2 Production yields of K isotopes. See caption of Fig. 1. The P_n values used are taken from Ref. 17. The cross-section scale is normalized to 0.35 mb for ^{44}K, assuming the same cross-section at the maximum of the yield distribution as that measured[12] for Sc.

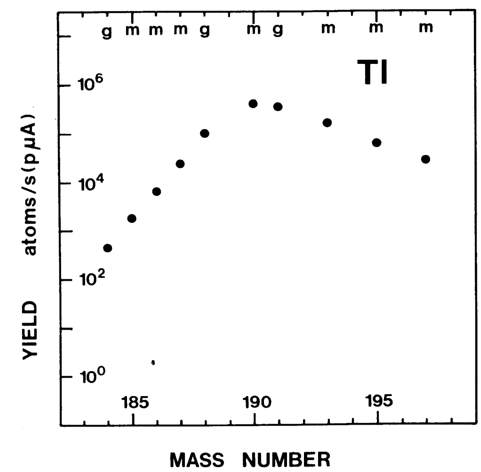

Fig. 3 Production yields of Tl isotopes. See caption of Fig. 1. No decay correction is applied to the points (see text). The letters m ang g indicate the metastable and the gound state, respectively. The same detection efficiency as for beta particles was used.

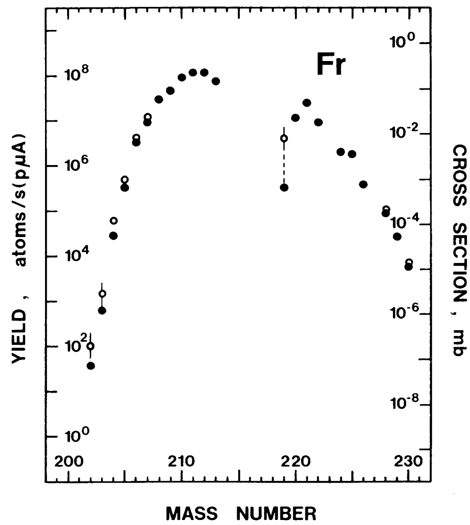

Fig. 4 Production yields of Fr isotopes. See caption of Fig. 1. The cross-section scale is normalized to 0.20 mb measured[13] for ^{212}Fr. The error bars are from the uncertainties in the μ value and the normal temperature variations of the target.

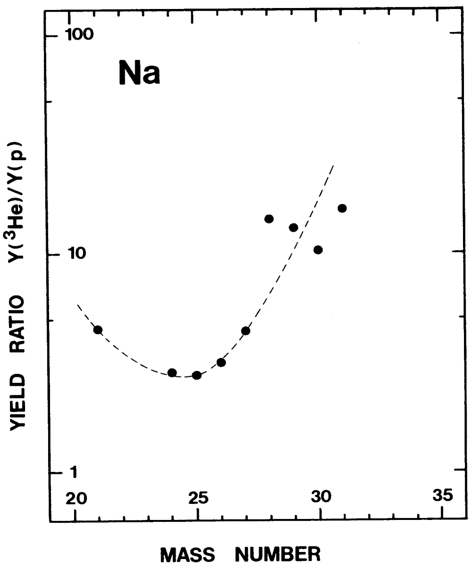

Fig. 5 Ratios of the ^{3}He to the proton-induced saturation yields of Na isotopes normalized to the same beam intensity.

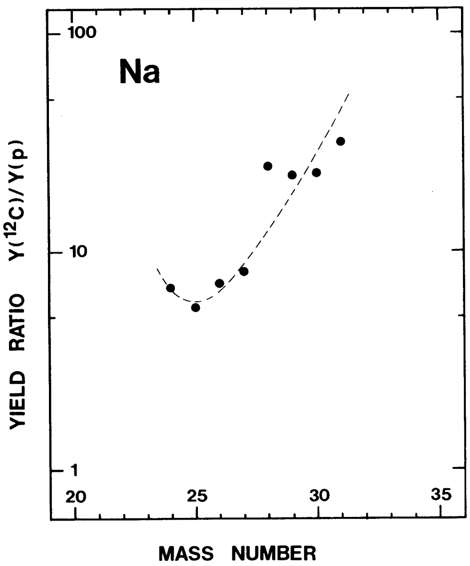

Fig. 6 Ratios of the ^{12}C to the proton-induced saturation yields of Na isotopes normalized to the same beam intensity.

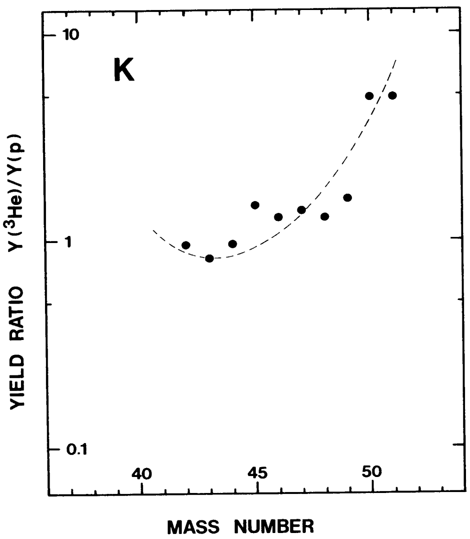

Fig. 7 Ratios of the K isotopes. See caption of Fig. 5.

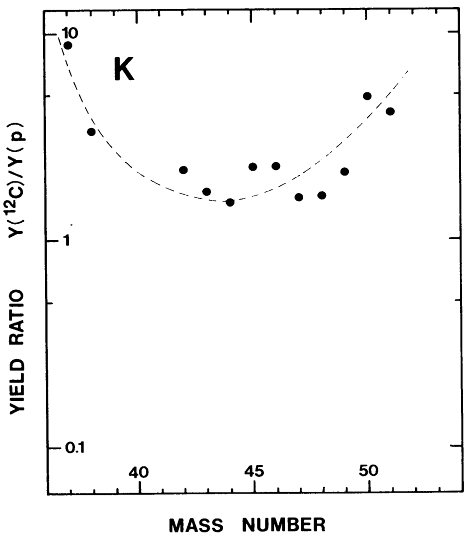

Fig. 8 Ratios of the K isotopes. See caption of Fig. 6.

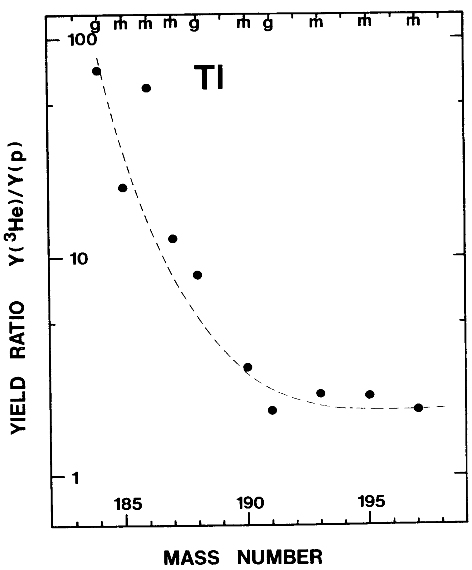

Fig. 9 Ratios of the Tl isotopes. See caption of Fig. 5. For the letters m and g see caption of Fig. 3.

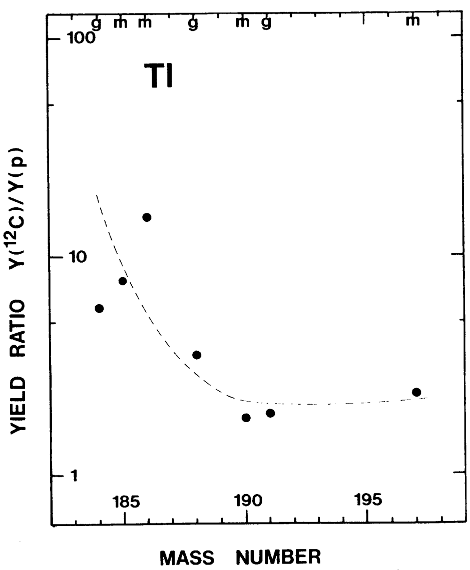

Fig. 10 Ratios of the Tl isotopes. See caption of Fig. 6. For the letters m and g see caption of Fig. 3.

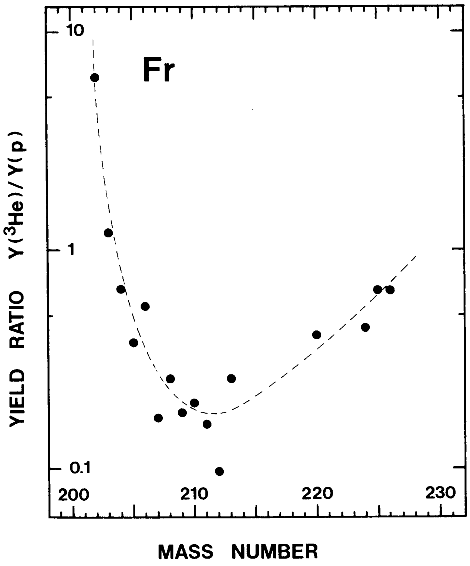

Fig. 11 Ratios of the Fr isotopes. See caption of Fig. 5.

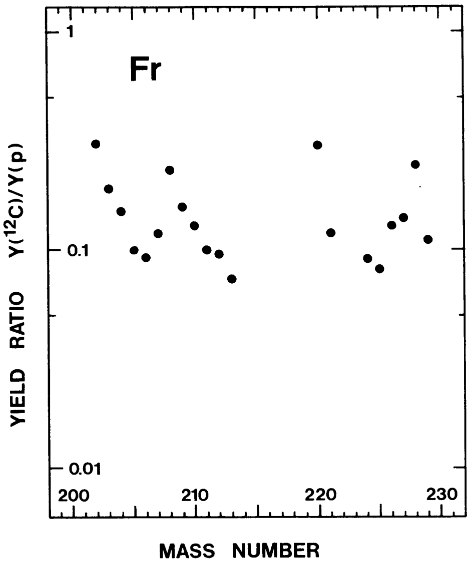

Fig. 12 Ratios of the Fr isotopes. See caption of Fig. 6.